Published in final edited form as:
J Periodontol. 2007 February ; 78(2): 273–281. doi:10.1902/jop.2007.060252.

Three-Dimensional Micro-Computed Tomographic Imaging of Alveolar Bone in Experimental Bone Loss or Repair

Chan Ho Park[*,†], **Zachary R. Abramson**[†], **Mario Taba Jr**[†], **Qiming Jin**[†], **Jia Chang**[‡], **Jaclynn M. Kreider**[§], **Steven A. Goldstein**[*,§], and **William V. Giannobile**[*,†,||]

[*] *Department of Biomedical Engineering, College of Engineering, University of Michigan, Ann Arbor, MI*

† *Department of Periodontics and Oral Medicine and Center for Craniofacial Regeneration, School of Dentistry, University of Michigan*

‡ *Department of Biologic and Materials Sciences, University of Michigan*

§ *Orthopaedic Research Laboratories, Department of Orthopaedic Surgery, University of Michigan*

|| *Michigan Center for Oral Health Research, Ann Arbor, MI*

Abstract

Background—Micro-computed tomography (micro-CT) offers significant potential for identifying mineralized structures. However, three-dimensional (3-D) micro-CT of alveolar bone has not been adapted readily for quantification. Moreover, conventional methods are not highly sensitive for analyzing bone loss or bone gain following periodontal disease or reconstructive therapy. The objective of this investigation was to develop a micro-CT methodology for quantifying tooth-supporting alveolar bone in 3-D following experimental preclinical situations of periodontitis or reconstructive therapy.

Methods—Experimental in vivo bone loss or regeneration situations were developed to validate the micro-CT imaging techniques. Twenty mature Sprague-Dawley rats were divided into two groups: bone loss (*Porphyromonas gingivalis* lipopolysaccharide-mediated bone resorption) and regenerative therapy. Micro-CT and software digitized specimens were reconstructed three-dimensionally for linear and volumetric parameter assessment of alveolar bone (linear bone height, bone volume, bone volume fraction, bone mineral content, and bone mineral density). Intra- and interexaminer reproducibility and reliability were compared for methodology validation.

Results—The results demonstrated high examiner reproducibility for linear and volumetric parameters with high intraclass correlation coefficient (ICC) and coefficient of variation (CV). The ICC showed that the methodology was highly reliable and reproducible (ICC >0.99; 95% confidence interval, 0.937 to 1.000; CV <1.5%), suggesting that 3-D measurements may provide better alveolar bone analysis than conventional 2-D methods.

Conclusions—The developed methods allow for highly accurate and reproducible static measurements of tooth-supporting alveolar bone following preclinical situations of bone destruction or regeneration. Future investigations should focus on using in vivo micro-CT imaging for real-time assessments of alveolar bone changes.

Keywords

Bone loss; computed tomography; periodontal disease; tissue engineering

Correspondence: Dr. William V. Giannobile, Michigan Center for Oral Health Research, University of Michigan Clinical Center, 24 Frank Lloyd Wright Dr., Lobby M, Box 422, Ann Arbor, MI 48106. Fax: 734/998-7228; e-mail: wgiannob@umich.edu.

Because of alveolar bone's non-uniformity and porous structure and its close proximity to dental structures, it is difficult to quantify. Current approaches that attempt to quantify alveolar bone include histomorphometry, two-dimensional (2-D) radiography, and more recently, micro-computed tomography (micro-CT).[1,2] Although histomorphometry provides high resolution and direct representations of alveolar bone levels, there are obvious limitations, such as tissue sample destruction and challenges in three dimensional (3-D) reconstruction.[3] Radiographic methods overcome many of these challenges by providing non-destructive 2-D imaging capabilities using sequential or serial images taken of alveolar bone and teeth while monitoring disease progression. However, the inconsistency in maintaining nearly identical alignment in successive radiographic images complicates this process.[4]

Micro-CT or medical CT is a non-destructive technique that can be used in 3-D to image specimens on the micron level and allows for computer-aided reorientation following image scanning, thus assuring nearly identical alignment.[1] Micro-CT for preclinical application provides higher spatial resolution images than medical or dental CT for clinical assessment.[5] Using this technique, compared to histologic sections, micro-CT scans show slight deviations at periodontal defects or in cases of alveolar bone loss.[5,6] In contrast, a study examining the reliability and accuracy of 2-D dental radiographs demonstrated differences of up to 25% between calculations quantifying alveolar bone from 2-D radiographs and 3-D CT scans.[7]

Conventional radiographic approaches assessing alveolar bone structure are limited by the fact that microarchitecture in 3-D cannot be inferred from isolated 2-D sections.[8] However, micro-CT can produce 3-D images of bone, allowing for detailed analysis of 3-D bone architecture and anisotropy. A study using micro-CT examined the mechanical behavior of bone in the attainment and maintenance of dental implant osseointegration. Assessment of the cancellous bone structure of maxillae and mandibulae from human cadavers revealed useful information about prognosis following implant reconstruction.[9]

Despite the advantages associated with micro-CT imaging, certain challenges have been issued in the reproducible osseous quantification of periodontal disease or post-regenerative therapy. Alveolar bone poses unique problems in its quantification because of the difficulty in distinguishing it from the surrounding dental hard tissues as a result of similarities in their attenuation of x-rays.[10] Typically, computer-assisted image analysis facilitates this process when the tissue of interest differs in density (and therefore, x-ray attenuation) from the surrounding structures. For example, in the quantification of trabecular bone, which differs significantly in density from non-bony constituents in the marrow space, an analysis algorithm can be devised to separate bone from non-bone elements accurately within the region of interest (ROI). In contrast, the anatomy and morphology of tooth-associated periodontal defects make density thresholding quite challenging. In periodontal tooth–bone defects, there is little difference in density between the tooth-supporting alveolar bone and the tooth roots, which are composed of hard tissue dentin and cementum separated by a thin fibrous tissue area (~150 to 200 μm) of intervening periodontal ligament.

In the present investigation, a reproducible method was developed for quantifying and assessing alveolar bone using high-resolution micro-CT employing an interactive image analysis technique to evaluate selected 3-D ROIs for tooth-supporting alveolar bone defects. This methodology is readily adaptable for preclinical assessments of linear and volumetric alveolar bone parameters following disease, trauma, or regeneration.

MATERIALS AND METHODS

Experimental Specimens

All animal procedures were performed under guidelines approved by the University of Michigan Unit for Laboratory Animal Medicine for the use of animals in research.

Experimental Bone Loss Group

Experimental alveolar bone loss was induced using *Porphyromonas gingivalis* lipopolysaccharide (*P. gingivalis* LPS). In brief, 12 adult male Sprague-Dawley rats (~250 g each)[¶] had experimental periodontitis induced by delivery of *P. gingivalis* W83 endotoxin[11] (10 μl of a 1.0 mg/ml preparation) by injection into the interdental gingivae between the maxillary first (M1), second (M2), and third molars (M3) and the mesial aspect of M1 under isoflurane general anesthesia. The administrations were repeated three times per week over an 8-week period. The injections were performed using custom-designed 0.375-inch × 33 gauge, 30° bevel needles attached to 50-μl syringes.[#] These 12 animals were divided into three subgroups: pretreatment baseline (N = 4), no disease post-protocol at 8 weeks (N = 4), and LPS-mediated bone loss (N = 4). The animals in the first group were sacrificed at baseline; the others were sacrificed at 8 weeks. Maxillary block biopsies were harvested, fixed in 10% neutral formalin for 2 days, and stored in 70% ethanol for scanning by micro-CT.

Experimental Bone Regeneration Group

An experimental alveolar bone defect model was used to measure bone repair following surgical creation of bone defects at the mesial root of the mandibular first molar, as described previously by Jin et al.[12] In brief, eight ~250-g athymic rats (Hsd:RH-rnu/rnu) (N = 4 per group) were anesthetized with ketamine[**] and xylazine[††] general anesthesia. Alveolar bone defect osteotomies were created by preparing an extraoral 2-cm superficial skin incision at the lower border of the mandible. The superficial fascia and underlying masseter muscle were separated with sharp dissection, and the ligamentary attachment of the masseter muscle to bone was severed at its inferior base; the masseter and periosteum were elevated from the bone to expose the buccal plate of the mandible. The oral mucosa on the superior wall of the surgically created osteotomy was identified, and its attachment to the intraoral keratinized gingival margin was maintained during defect preparation. The bone overlying the mandibular first molar was removed with a high-speed handpiece under saline irrigation while visualizing with a surgical microscope.[‡‡] The distal root of the first molar was denuded of periodontal ligament, overlying cementum, and superficial dentin. The defects measured ~0.3 × 0.2 × 0.15 cm. Polylactic glycolic acid scaffolds seeded with 2.5×10^5 non-transduced cells (scaffold-alone control) or 2.5×10^5 genetically modified stem cells were placed in the defects, as described previously.[13] The internal wounds were approximated with bioabsorbable 5-0 chromic gut sutures, and the external skin incisions were closed with surgical staples. The animals were administered supplemental antibiotics (ampicillin and 268 μg/ml of drinking water) daily for up to 14 days. At 5 weeks, the animals were sacrificed, and mandibular block biopsies were harvested, fixed in 10% neutral formalin for 2 days, and stored in 70% ethanol for scanning by micro-CT.

[¶]Harlan World Headquarters, Indianapolis, IN.
[#]Hamilton, Reno, NV.
[**]Ketaset, Fort Dodge Animal Health, Fort Dodge, IA.
[††]AnaSet, Lloyd Laboratories, Shenandoah, IA.
[‡‡]SMZ 1000, Nikon, Melville, NY.

Micro-CT Instrumentation and Image Capture

Allmaxillary and mandibular block biopsies were subjected to micro-CT image capture as described below. The main components of the cone-beam scanner[§§] for alveolar bone application are shown in Figure 1. The x-ray generator was operated at an accelerated potential of 80 kV with a beam current of 80 μA. The x-ray source combines with a 2-D detector operating with a shutter speed of 1,100 ms, which produces images with a voxel size of $18\times18\times18\mu m^3$. Bone mineral density unit(mg/cc) is calculated and determined with an internal reference in micro-CT units.

The 3-D volume viewer and analyzer software[||||] was used for the visualization and quantification of 2-D and 3-D data on a personal computer output. Post-processing images were colorized with a software program.[¶¶]

Linear and Volumetric Alveolar Bone Measurements

Linear measurements: Linear measurements were taken (in millimeters) from the cemento-enamel junction (CEJ) to the alveolar bone crest (ABC) in the interdental region between the first and second molars (M1-M2) or the second and third molars (M2-M3). All images were reoriented such that the CEJ and the root apex (RA) appeared in the micro-CT slice that was to be analyzed. Measurements of root lengths (RLs) from the CEJ to the RA also were taken (in millimeters) to assess the percentage of vertical bone remaining (Fig. 2B).

To assess the amount of regenerated bone tissues in the reconstructive therapy group, the exposed RL of the distal root of M1(d-M1) was measured (in millimeters). The linear fractions (as noted in Equation 3) represent the linear amount of regenerated bone tissue covering the surgically created dehiscence lesion.

Volumetric micro-CT measurements: Volumetric measurements were carried out following the selection of a 3-D ROI. Two examiners (CHP and ZA) were guided by morphological landmarks when drawing ROIs to ensure repeatability. Although artificial landmarks could have been placed prior to the scanning of the images, it was more convenient and more reproducible to use given morphological features (e.g., outer root prominences and root furcations). In the case of periodontal defects resulting from experimental periodontitis, most bone loss was noted around the roots of the teeth, below the roofs of the furcations (ROFs) and above the RA. Our method takes advantage of this feature by using the ROFs and the RAs as references identifying the borders of the ROIs (Fig. 2A).

The most mesial root of M1 (m-M1) and the most distal root of M3 (d-M3) served as endpoint landmark borders because they were the most consistent among specimens. Thus, the reorientation of specimens from examiner to examiner relies on the capturing of these landmarks, which essentially maximizes the ROI of the alveolar bone housing the alveolus. The critical reorientation of 3-D reconstructed images provided the reproducible and reliable criteria to quantify and assess alveolar bone. In contrast, based on the examination of maxillae with the orientation stated above, the relative heights of the ROFs varied greatly. Thus, in all cases it was not feasible to start with one specific furcation each time. Consequently, contours were drawn immediately upon scrolling through the top of a furcation landmark (Fig. 2A).

[§§] Model Pxs5-928EA, GE Healthcare, London, ON.
[||||] eXplore MicroView v.2.0, Analysis Plus, GE Healthcare.
[¶¶] Adobe Photoshop CS2 v.9.0, Adobe Systems, San Jose, CA.

Using the landmarks RA, ROF, and RL, desired region contours were drawn at regular intervals (Fig. 2A and equations 1 through 3). The objectives in drawing these contours were to maximize the quantification of bone, minimize the inclusion of tooth roots, and use as many reproducible landmarks as possible. All contours were drawn beginning immediately below the ROFs in the coronal plane and moving in the apical direction. Using an advanced ROI tool, 2-D contours were drawn at regular intervals (every eight data planes), depending on the variability between planes; greater variability between planes required contours to be drawn at smaller intervals (one to two planes). Contours were drawn until reaching the apices ofm-M1and d-M3. Next, a 3-DROI was generated by the software based on the resultant 2-D contours (Figs. 2A and 2C). Finally, volumetric alveolar bone parameters of bone volume (BV), bone volume fraction (BVF), bone mineral content (BMC), and bone mineral density (BMD) in the volume of selected and contour-drawn ROIs were determined (Fig. 2C) using equations 4 and 5.

Equations used in image measures: ***Equation 1:*** Percent remaining bone (%) = ([root length − CEJ-ABC]/root length) × 100, where CEJ - ABC= the distance from the CEJ to ABC.

Equation 2: Root length = (M1 + M2)/2 and (M2 + M3)/2, where M*i* = the distance of the i^{th} molar root from CEJ to RA.

Equation 3: Linear fraction = length of exposed d-M1 root/total length of d-M1 root, where the total length of d-M1 root = the distance of the d-M1 root from the CEJ to RA.

Equation 4: Bone volume fraction = remaining bone volume in volume of interest/volume of interest.

Equation 5: Bone mineral content = bone mineral density × volume of interest.

Examiner Reliability and Statistical Analysis

Validation measures were conducted for linear and volumetric micro-CT measurements. For the linear validation, eight samples were analyzed by two independent examiners (CHP and ZA). After 24 hours, linear distance measurements were repeated by both examiners to assess inter- and intraexaminer variability. Analogously, for the volumetric validation, one image was taken, and six planes were selected for analysis: two planes near the crowns, two near the apices, and two in the mid-portion of the roots. The examiners independently prepared contours in the selected planes to assess volumetric parameters BV, BVF, BMC, and BMD according to equations 4 and 5. Again, all volumetric measurements were repeated after 24 hours by both examiners to assess inter- and intraexaminer variability. In addition, one image was chosen and analyzed completely by each examiner twice to obtain agreements.

Mean values were generated for each of the groups evaluated. The coded specimens were analyzed using one-way analysis of variance and Bonferroni multiple comparison test to measure statistical differences among groups. The reliability and reproducibility provided the intraclass correlation coefficient (ICC). Values for ICC range from 0 to 1. When ICCs are closer to 1, reliability and reproducibility are stronger; ICC values >0.75 show good reliability.[14] The values were calculated with single measurements from a two-way random model and absolute agreement type of ICC in a statistical software package.[##] Coefficient of variation (CV % = [SD/its mean value] × 100) can describe the reproducibility of measurement as a precision error.[15] The reproducibility and repeatability of duplicate micro-CT scans and the developed methodology were calculated statistically using CV. One sample was scanned once

[##]SPSS v.12, SPSS, Chicago, IL.

a day for 3 days. All measured volumetric results from the scans and software[***] and the calibration measurements were evaluated with a statistical software package.[†††]

RESULTS

The methodology of image capture, orientation, landmark identification, and measures of linear bone change, BV, BVF, BMC, and BMD were reproducible; the methods used for measurement are highlighted in Figures 2 and 3. Two-dimensional and 3-Dtopographical alterations in bone levels are shown in Figure 4.

Linear Micro-CT Measurements

In the alveolar bone loss specimens, linear measurements in the interdental regions M1-M2 and M2-M3 demonstrated significant differences between the healthy specimens and those that had *P. gingivalis* LPS-induced periodontitis. We measured CEJ–ABC distances at baseline and follow-up (Fig. 3). As Figure 3A reveals, there was no significant difference between values recorded at baseline and those recorded at 8 weeks in the group with no disease ($P > 0.05$). However, when diseased periodontia were compared to healthy specimens at follow-up, statistically significant differences were found ($P < 0.05$).

In the reconstructive therapy group, the residual tooth root exposure was reduced significantly by genetically modified cell therapy compared to the control group (Fig. 3D; $P < 0.05$). Colorized images depict bone gain following reconstructive therapy over the previously debrided tooth root surface (Figs. 4H through 4I; $P < 0.01$).

Volumetric Micro-CT Measurements

Using this methodology, we could obtain the volumetric parameters for multiple bone loss indices including bone volume, bone volume fraction, bone mineral content, and bone mineral density. In the bone loss specimens, no statistically significant differences of volumetric bone parameters were found between the baseline and follow-up healthy (control) group ($P > 0.05$). However, LPS-induced experimental periodontitis led to robust and statistically significant bone loss as compared to the control group (Figs. 3B and 3C; $P < 0.05$) for the volumetric parameters BMD and BVF. As a result, among both experimental groups (disease or repair) we could quantitatively determine the amount of bone change in both 2-D and 3-D (Figs. 3 and 4).

Reliability

The values of ICC for continuous agreement analysis and for reliability and reproducibility of measurements was high. In summary, both examiners showed very high inter- and intraexaminer agreement, highlighting the reliability and reproducibility of this method (Table 1). Highly sensitive, reliable, and reproducible measures were shown for the intraclass correlation coefficient (ICC >0.99; 95% confidence interval [CI] = 0.937 to 1.000), leading to a standardized measurement method. CV demonstrated precise error for the reproducibility of developed volumetric measurements. CV was <1.5% in inter- and intraexaminer calibrations, and this methodology has very high reproducibility and reliability of measurement. Moreover, micro-CT scanning showed high reproducibility and repeatability with very low precision errors. BVF and BMD had 0.837% and 2.0618% precision errors, respectively. The experimental preclinical situations revealed measurable disease progression in the case of *P. gingivalis* LPS-mediated periodontitis or alveolar bone repair using regenerative cell therapy (Table 1).

[***]MicroView.
[†††]SPSS v.12, SPSS.

DISCUSSION

Traditionally, 2-D radiographic images and histomorphometry have provided linear data to enable investigators to make quantitative measurements associated with alveolar bone affected by periodontitis or following regenerative therapy.[16,17] Although new technologies are available for 3-D assessment of bone volume, in general, approaches still measure 2-D images linearly after projection from 3-D real structures.[18,19] These methods have limitations, such as the accuracy or the precision of measurements. [20,21] Micro-CT techniques have the potential to overcome these limitations and provide a more accurate quantification method for 3-D assessment of bone.[22,23] The volumetric technique demonstrated accurate and precise amounts of remaining bone in cases of no disease, disease, and postreconstructive therapy (Fig. 4). Furthermore, intra- and interexaminer reliability data demonstrate no significant differences between examiners, suggesting that the method is reproducible in terms of measures of captured and reoriented images. In fact, following the inclusion of a third examiner also provided high agreement of reproducibility in image capture of differences <3% (data not shown). Our reorientation criteria and methodology provided high reliability and reproducibility of quantification assessments and volumetric parameters (BV, BVF, BMC, and BMD), although micro- CT scanning introduced variability in images.

Although histologic techniques provide similar spatial data in calcified and decalcified tissues, micro-CT enables detailed 3-D microarchitecture visualization without tissue processing artifactual alterations in anatomical tissue structure. The correspondence between histologic and micro-CT data was explored by comparing digitized images from histologic sections to matching micro-CT planes; both methods have qualitative similarity (6 to 8 μm thick and 18 μm thick; Figs. 4C and 4D).[5,24] Although cells cannot be observed in micro-CT images, discrete changes in alveolar bone morphology and trabeculation can be assessed three-dimensionally (Fig. 4).[3,25,26] High resolution 3-D micro-CT images provide the advantage of observing tissues without tissue-processing treatments that can result in the distortion of osseous structures.[27,28]

Wilensky et al.[10] showed that micro-CT imaging could overcome several problems of previous 2-D approaches and demonstrated the verification of the quantification of bone loss following periodontitis. Central to our method was the use of enhanced image analysis that provided the technological abilities to overcome many of the previous challenges in the quantification of alveolar bone.[17,29]

CONCLUSIONS

These approaches for quantitative assessment of periodontal osseous structures demonstrated the reliability and reproducibility of 3-D micro-CT measurements of alveolar bone. Our selected landmarks for quantification of alveolar bone (ROF, the most distal end of molar roots, and tangent line between roots on the coronal plane for landmark detection of ROI) provided critical criteria and reproducibility to measure volumetric osseous parameters. The measurements demonstrated strong agreement between examiners and significant reliability and reproducibility (ICC- >0.99 and CV <1.5%). Therefore, this methodology can serve as a standard for static bone assessment of disease progression and alveolar bone regeneration with high accuracy.

The use of micro-CT assessment and associated imaging algorithms provide effective 3-D visualization and image analysis of the bone–tooth interface that complement periodontal, craniofacial, and orthopedic investigations. Future studies should focus on using in vivo micro-CT imaging approaches for real-time assessments of alveolar bone changes that could lead to dynamic, rather than static, measures of osseous change.

Acknowledgements

The authors appreciate the technical assistance of Christoph Ramseier, James Sugai, Nancy Chen, and Drew DiGiore, Department of Periodontics and Oral Medicine, University of Michigan. Statistical consultation by Dr. Charles Kowalski, Department of Biologic and Materials Sciences, University of Michigan, is appreciated. The cone-beam micro-CT scanner used in this study (model Pxs5-928EA) was developed by General Electric Enhanced Vision Systems, GE Healthcare, London, Ontario, Canada. This study was funded by the National Institutes of Health (NIH)/ National Institute of Dental and Craniofacial Research (NIDCR) (NIDCR grants R01-DE13397, R01-DE015384, and R21-DE016619 to WVG and NIH P30-AR46024 to SAG).

References

1. Hamada Y, Kondoh T, Noguchi K, et al. Application of limited cone beam computed tomography to clinical assessment of alveolar bone grafting: A preliminary report. Cleft Palate Craniofac J 2005;42:128–137. [PubMed: 15748103]
2. Hausmann E. Radiographic and digital imaging in periodontal practice. J Periodontol 2000;71:497–503. [PubMed: 10776940]
3. Bernhardt R, van den Dolder J, Bierbaum S, et al. Osteoconductive modifications of Ti-implants in a goat defect model: Characterization of bone growth with SR muCT and histology. Biomaterials 2005;26:3009–3019. [PubMed: 15603796]
4. Rawlinson A, Elcock C, Cheung A, et al. An in-vitro and in-vivo methodology study of alveolar bone measurement using extra-oral radiographic alignment apparatus, Image Pro-Plus software and a subtraction programme. J Dent 2005;33:781–788. [PubMed: 15922503]
5. Van Oossterwyck H, Duyck J, Vander Sloten J, et al. Use of microfocus computerized tomography as a new technique for characterizing bone tissue around oral implants. J Oral Implantol 2000;26:5–12. [PubMed: 11831302]
6. Mengel R, Candir M, Shiratori K, Flores-de-Jacoby L. Digital volume tomography in the diagnosis of periodontal defects: An in vitro study on native pig and human mandibles. J Periodontol 2005;76:665–673. [PubMed: 15898924]
7. Rosenstein SW, Long RE Jr, Dado DV, Vinson B, Alder ME. Comparison of 2-D calculations from periapical and occlusal radiographs versus 3-D calculations from CAT scans in determining bone support for cleft-adjacent teeth following early alveolar bone grafts. Cleft Palate Craniofac J 1997;34:199–205. [PubMed: 9167069]
8. Feldkamp LA, Goldstein SA, Parfitt AM, Jesion G, Kleerekoper M. The direct examination of three-dimensional bone architecture in vitro by computed tomography. J Bone Miner Res 1989;4:3–11. [PubMed: 2718776]
9. Fanuscu MI, Chang TL. Three-dimensional morphometric analysis of human cadaver bone: Microstructural data from maxilla and mandible. Clin Oral Implants Res 2004;15:213–218. [PubMed: 15008933]
10. Wilensky A, Gabet Y, Yumoto H, Houri-Haddad Y, Shapira L. Three-dimensional quantification of alveolar bone loss in *Porphyromonas gingivalis*-infected mice using micro-computed tomography. J Periodontol 2005;76:1282–1286. [PubMed: 16101359]
11. Taba MJ, Huffer HH, Shelburne CE, et al. Gene delivery of TNFR:Fc by adeno-associated virus vector blocks progression of periodontitis. Mol Ther 2005;11(Suppl 1):S262.
12. Jin Q, Anusaksathien O, Webb SA, Printz MA, Giannobile WV. Engineering of tooth-supporting structures by delivery of PDGF gene therapy vectors. Mol Ther 2004;9:519–526. [PubMed: 15093182]
13. Jin QM, Zhao M, Webb SA, et al. Cementum engineering with three-dimensional polymer scaffolds. J Biomed Mater Res A 2003;67:54–60. [PubMed: 14517861]
14. Zhu F, Sarkar S, Kaitwatcharachai C, et al. Methods and reproducibility of measurement of resistivity in the calf using regional bioimpedance analysis. Blood Purif 2003;21:131–136. [PubMed: 12596759]
15. Kohler T, Beyeler M, Webster D, Muller R. Compartmental bone morphometry in the mouse femur: Reproducibility and resolution dependence of microtomographic measurements. Calcif Tissue Int 2005;77:281–290. [PubMed: 16283571]

16. Reddy MS. Radiographic alveolar bone change as an outcome measure for therapies that inhibit bone loss or foster bone gain. J Int Acad Periodontol 2005;7:175–188. [PubMed: 16248274]

17. Misch KA, Yi ES, Sarment DP. Accuracy of cone beam computed tomography for periodontal defect measurements. J Periodontol 2006;77:1261–1266. [PubMed: 16805691]

18. Chen SK, Pan JH, Chen CM, Jeng JY. Accuracy of supported root ratio estimation from projected length and area using digital radiographs. J Periodontol 2004;75:866–871. [PubMed: 15295954]

19. Wolf B, von Bethlenfalvy E, Hassfeld S, Staehle HJ, Eickholz P. Reliability of assessing interproximal bone loss by digital radiography: Intrabony defects. J Clin Periodontol 2001;28:869–878. [PubMed: 11493358]

20. Sarment DP, Sukovic P, Clinthorne N. Accuracy of implant placement with a stereolithographic surgical guide. Int J Oral Maxillofac Implants 2003;18:571–577. [PubMed: 12939011]

21. Bianchi J, Fiorellini JP, Howell TH, et al. Measuring the efficacy of rhBMP-2 to regenerate bone: A radiographic study using a commercially available software program. Int J Periodontics Restorative Dent 2004;24:579–587. [PubMed: 15626320]

22. Sant'Anna EF, Gomez DF, Sumner DR, et al. Micro-computed tomography evaluation of the glenoid fossa and mandibular condyle bone after bilateral vertical ramus mandibular distraction in a canine model. J Craniofac Surg 2006;17:111–119. [PubMed: 16432418]

23. Luo G, Kinney JH, Kaufman JJ, et al. Relationship between plain radiographic patterns and three-dimensional trabecular architecture in the human calcaneus. Osteoporos Int 1999;9:339–345. [PubMed: 10550451]

24. Hirabayashi S, Umamoto N, Tachi M, et al. Optimized 3-D CT scan protocol for longitudinal morphological estimation in craniofacial surgery. J Craniofac Surg 2001;12:136–140. [PubMed: 11314623]

25. Postnov AA, Vinogradov AV, Van Dyck D, Saveliev SV, De Clerck NM. Quantitative analysis of bone mineral content by x-ray microtomography. Physiol Meas 2003;24:165–178. [PubMed: 12636194]

26. Gauthier O, Muller R, von Stechow D, et al. In vivo bone regeneration with injectable calcium phosphate biomaterial: A three-dimensional micro-computed tomographic, biomechanical and SEM study. Biomaterials 2005;26:5444–5453. [PubMed: 15860201]

27. Johnson AJW, Wojtowicz AM, Dellinger JG, et al. 3D tissue distribution patterns characterized by micro-CT. Mat Res Soc Symp Proc 2004;EXS-1:F5.18.11–F15.18.13.

28. Yang J, Pham SM, Crabbe DL. Effects of oestrogen deficiency on rat mandibular and tibial microarchitecture. Dentomaxillofac Radiol 2003;32:247–251. [PubMed: 13679356]

29. Jones AC, Sakellariou A, Limaye A, et al. Investigation of microstructural features in regenerating bone using micro computed tomography. J Mater Sci Mater Med 2004;15:529–532. [PubMed: 15332630]

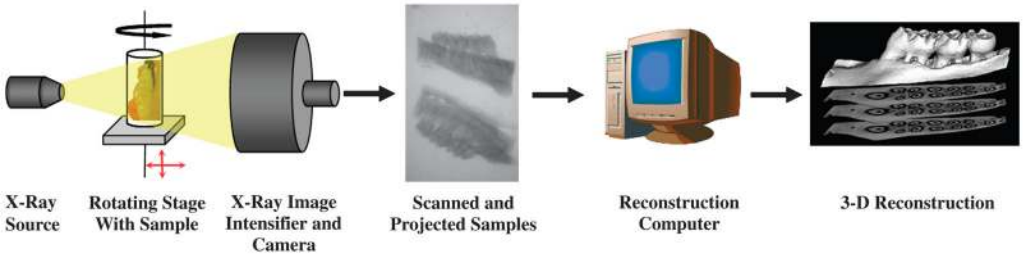

Figure 1.
Cone-beam micro-CT for assessment of alveolar bone. Specimens are exposed to polychromatic x-rays on a rotating stage. X-rays that penetrate the mandible or maxilla pass through an image intensifier and are captured by a camera, producing 2-D slices of 18-μm thickness. Finally, cross-sectional images are reconstructed into a 3-D structure by a host computer.

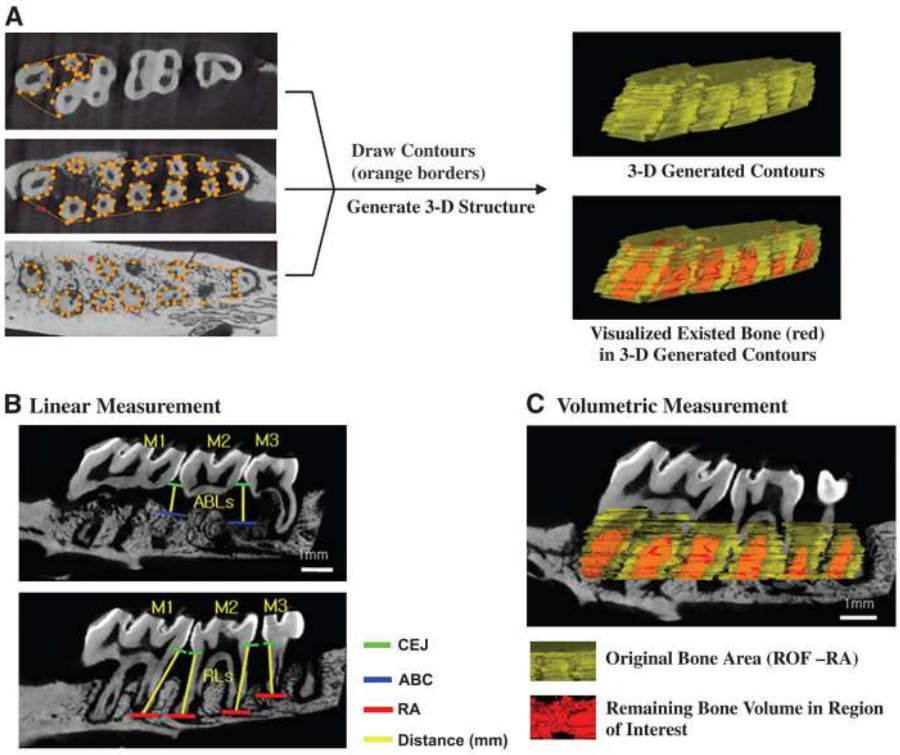

Figure 2.

Method for creating 3-D ROIs used in analysis of alveolar bone. **A)** Two-dimensional contours are drawn at regular intervals from the ROFs to the RAs. Once all contours are drawn, a 3-D ROI is generated for reconstruction. **B)** Linear measurements are taken of alveolar bone loss (ABL) in the interdental space from the CEJ to ABC and RLs from the CEJ to RA (in millimeters). **C)** Volumetric measurement with 3-D generated ROIs. Software assesses the amount of bone and analyzes volumetric parameters in the volume of interest that are 3-D generated contours.

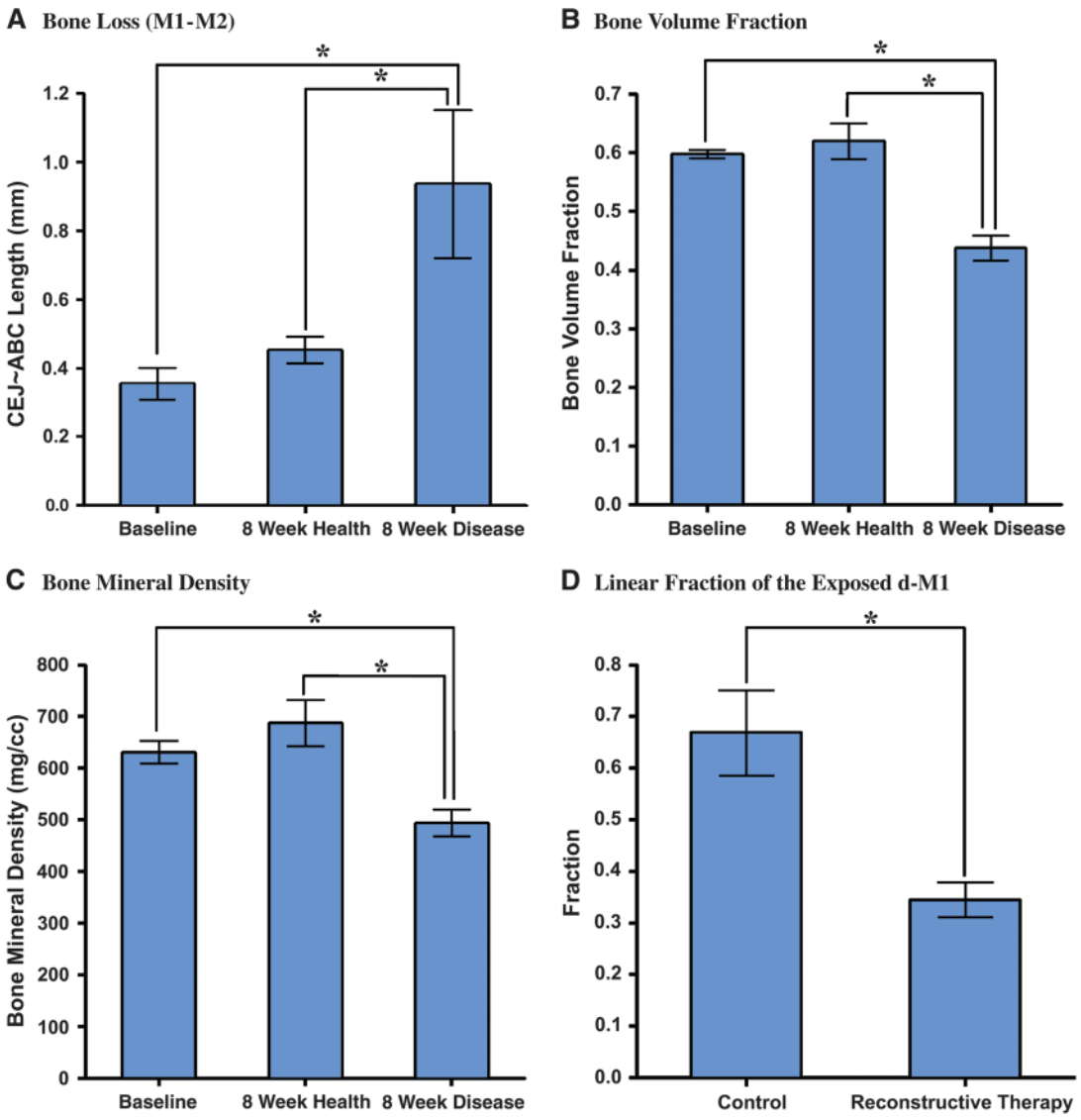

Figure 3.

Linear measurements of interdental CEJ-ABC and volumetric measurement of ROF-RA. The analyses of linear measurements and volumetric measurements at baseline and among healthy and diseased groups. **A)** Bone loss distances represented as CEJ-ABC length. Bone loss in the *P. gingivalis* LPS-induced periodontitis group was significantly greater than at baseline and in the group with no disease. In the volumetric measurements, significant differences also could be observed between diseased and other groups in bone volume fraction **(B)**, bone mineral content (not shown), and bone mineral density **(C). D)** After reconstructive cell therapy, exposed defects at the distal root areas of M1 were measured linearly as a proportion of the total RL. There was a significant difference between non-transduced and transduced cell therapy groups. **P* <0.05.

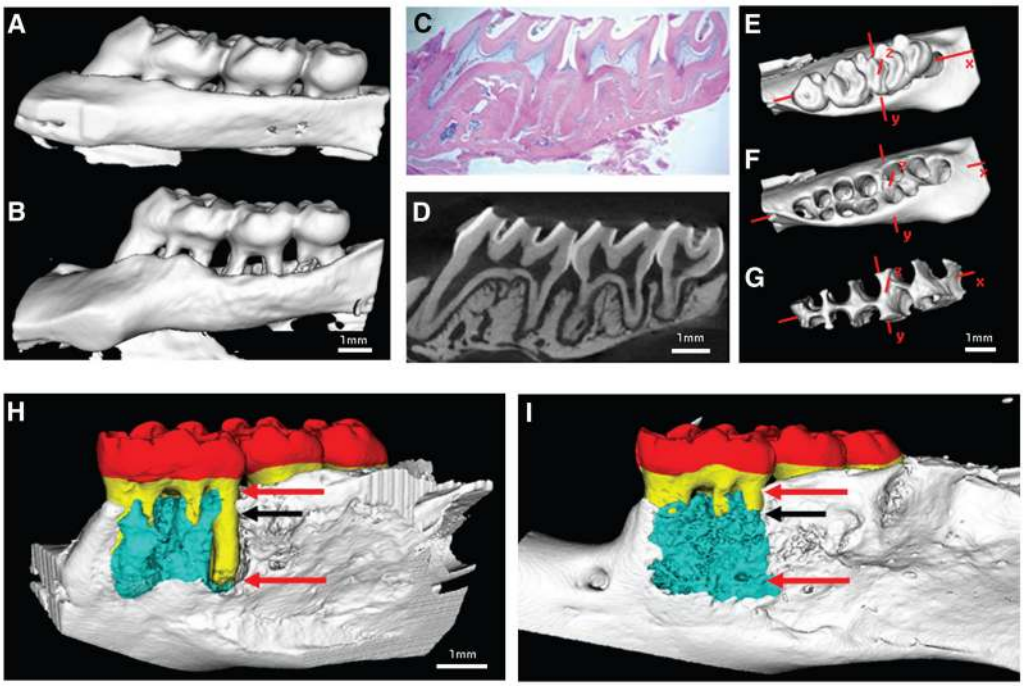

Figure 4.

Representative specimens displaying bone loss in healthy **(A)** and diseased **(B)** periodontia. Cross-sectional histologic image with hematoxylin and eosin (H&E) staining **(C)** and the corresponding micro-CT slice **(D)** demonstrate similarity of sections. Three-dimensional isosurfaces in a Cartesian coordinate system display an extracted rat maxilla including all three molars **(E)**, rat maxilla with teeth extracted digitally **(F)**, and alveolar bone within a preselected ROI used in bone volume determination **(G)**. Surgically-induced dehiscence osseous defects in a mandibular defect biopsied at 5 weeks post-therapy. **(H)** Control group. **(I)** Reconstructive therapy group demonstrating bone repair over the previously dehisced lesion of the M1 distal root. Red = crown; yellow = tooth root; blue = regenerated bone; red arrows = standardized root fenestration osseous defects; black arrows = top side of the scaffold implanted site on the osseous defect.

Table 1

Statistical Results for Reliability and Reproducibility in Developed Methodology With ICC and CV

	ICC	CV (%)	95% CI	
			Lower Boundary	Upper Boundary
Intraexaminer calibration				
Examiner 1	0.999	1.2	0.937	1.000
Examiner 2	0.997	0.7	0.980	1.000
Interexaminer calibration	0.999	1.4	0.990	1.000